Multivariate pattern analysis reveals resting-state EEG biomarkers in fibromyalgia

Dino Soldic[1,3], María Carmen Martín-Buro[1,3], David López-García[2], Ana Belén del Pino[1,3], Roberto Fernandes-Magalhaes[1,3], David Ferrera[1,3], Irene Peláez[1,3] and Francisco Mercado[1,3]

Author affiliations:

1 Department of Psychology, Faculty of Health Sciences, Rey Juan Carlos University, 28922 Alcorcón, Madrid, Spain

2 Mind, Brain and Behavior Research Center, 18011 Granada, Andalucía, Spain.

3 Research group in Cognitive Neuroscience, Pain and Rehabilitation (NECODOR), Rey Juan Carlos University, 28922 Alcorcón, Madrid, Spain

Correspondence to: Francisco Mercado

Department of Psychology, Faculty of Health Sciences, Rey Juan Carlos University, 28922 Alcorcón, Madrid, Spain

E-mail: francisco.mercado@urjc.es

Keywords: chronic pain; pain processing; frequency bands; neural markers; multivariate analysis; cognitive control; support vector machine; discriminant analysis

Introduction

Fibromyalgia (FM) affects 2-8% of the population, predominantly women [11]. The syndrome involves widespread musculoskeletal pain and hypersensitivity, also affecting neurological, cognitive, and affective domains [17,20,21,24,44,45]. Its controversial neurobiological basis and variable symptoms, such as fatigue and insomnia, complicate diagnosis and treatment despite established criteria [36,54,55], driving research to employ electromagnetic techniques aimed at understanding its neurobiological mechanisms. Electroencephalography (EEG) is especially useful, as it can detect abnormalities in basal brain function even during resting-state (RS) conditions. In this line, anomalous cortical activity in FM has been shown to be more concentrated in parietal regions within theta, alpha, and beta bands [40]. Additionally, Fallon et al. [17] observed increased theta activity associated with heightened pain perception, localized via source reconstruction to the anterior cingulate, medial prefrontal, and dorsolateral prefrontal cortices. Other studies report diminished connectivity between default mode network regions and somatosensory cortices in the theta band [10,32], a pattern linked to hypersensitive neural processing in FM [40].

Although several studies have reported EEG abnormalities in FM, findings remain inconsistent regarding the underlying neural mechanisms. González-Villar et al. [25] observed increased alpha and beta activity in frontal regions, possibly reflecting dysregulated top-down control contributing to FM patients' attentional and cognitive deficits [18,19]. Furthermore, emotional states often influence these processes, with anxiety being significantly more prevalent and severe in FM than in healthy controls (HC) [22,29], often leading to a marked reduction in quality of life [8,9].

Beyond emotional factors, cortical alterations may reflect long-term consequences of chronic pain. In this line, electrophysiological studies have linked FM symptom duration to increased

theta power in frontal and parietal regions, indicating that prolonged exposure to pain and fatigue leads to alterations as FM progresses [53]. Furthermore, frontocentral activity alterations associated with ongoing tonic pain and fatigue support the notion of cumulative neural impact in prolonged FM exposure [2,17].

Given the syndrome's variability and complexity, machine learning (ML) analysis methods have gained popularity for their ability to improve statistical sensitivity and specificity by detecting subtle signal changes often overlooked by conventional analyses, thereby preserving valuable information [37,39,51,58]. For instance, López-Solà et al. [38] identified new cortical regions involved in FM using multivariate pattern analysis of functional magnetic resonance imaging data. Additionally, linear support vector machine and linear discriminant analysis effectively differentiated epilepsy and schizophrenia patients from HC in RS-EEG conditions [1,15,47]. Furthermore, Hsiao et al. [31], integrating power spectral density, functional connectivity, and psychometric variables predicted differences in heat pain sensitivity, highlighting the potential of ML to model pain processing mechanisms using RS-EEG features.

Despite their potential, such approaches have yet to be applied to FM populations, highlighting the need for methods that deepen our understanding of FM's neurobiological foundations and reliably differentiate patients from HC, while accounting for clinical symptoms. Therefore, this study aims to: 1) differentiate RS-EEG signals of FM patients and HC across frequency bands leveraging state and trait anxiety scores; 2) distinguish patients based on symptom duration; and 3) identify neural activity in key scalp regions contributing to classification.

Materials and methods

Paradigm and data acquisition

Participants

Fifty-one women participated in the study, comprising 25 fibromyalgia (FM) patients (mean age ± SD = 52.15 ± 6.06) and 26 healthy controls (HC; mean age ± SD = 48.73 ± 7.01), with ages ranging from 35 to 65 years. FM patients were recruited through the Fibromyalgia and Chronic Fatigue Syndrome Association of Móstoles (AFINSYFACRO) and the Madrid Fibromyalgia Association (AFIBROM). They were evaluated by rheumatologists from hospitals in the Community of Madrid and met the diagnostic criteria defined by the American College of Rheumatology [54,56]. HC were recruited through posters displayed around the Faculty of Health Sciences at Rey Juan Carlos University, as well as through emails sent to the entire university community. Participants with neurological disorders, metabolic alterations, cognitive impairments, substance abuse or dependence, or psychiatric disorders were excluded from the study. FM patients had a mean diagnosis duration of 94 months (SD = 50.77). Prescribed medications and therapeutic interventions were continued due to medical recommendations and ethical guidelines.

Procedure

The study adhered to the ethical standards of the World Medical Association's Helsinki Declaration (1964) and its later amendments. All participants provided written informed consent, and the study was approved by the Rey Juan Carlos University Research Ethics Committee (ref: 201000100011550).

Upon arrival at the Laboratory of Cognitive Neuroscience (Faculty of Health Sciences, Rey Juan Carlos University), participants completed a sociodemographic and clinical

questionnaire. Sociodemographic data included age, educational level, and regular medication use. Additionally, FM patients reported the duration of their diagnosis in months. FM and HC groups were matched for age [t (49) = 1.625, p = 0.111, d = 0.455] and educational level [$\chi^2(4) = 8.106$, $p = 0.088$, $V = 0.399$].

Given the close relationship between anxiety and FM [22], the State-Trait Anxiety Inventory (STAI) [49] was administered to assess both state (STAI-S) and trait (STAI-T) anxiety. Sociodemographic and clinical data are presented in Table 1.

Table 1 Sociodemographic and clinical data

	Fibromyalgia (*N* = 25)	Healthy Control (*N* = 26)	*T*-test/ chi square	Significance level	Effect size
Age (years. M ± SD)	51.60 ± 5.47	48.73 ± 7.01	$t = 1.625$	$p = 0.111$	$d = 0.455$
Educational level			$\chi^2 = 8.106$	$p = 0.088$	$V = 0.399$
None, *N* (%)	3 (5.9%)	0 (0%)	-	-	-
Primary school, *N* (%)	11 (21.6%)	8 (15.7%)	-	-	-
Secondary school, *N* (%)	7 (13.7%)	6 (11.8%)	-	-	-
High school, *N* (%)	3 (5.9%)	11 (21.6%)	-	-	-
Bachelor's degree, *N* (%)	1 (2%)	1 (2%)	-	-	-
Diagnosis history (months. M ± SD)	94 ± 50.77	-	-	-	-
Diagnosis history (months. Median)	92	-	-	-	-
Medication					
Antidepressants, *N* (%)	14 (56%)	0 (0%)	-	-	-
Anxiolytics, *N* (%)	6 (24%)	0 (0%)	-	-	-
Analgesics, *N* (%)	10 (40%)	0 (0%)	-	-	-
Antiepileptics/Psycholeptics, *N* (%)	4 (16%)	0 (0%)	-	-	-
Other, *N* (%)	9 (36%)	0 (0%)	-	-	-
Trait anxiety (STAI-T percentile. M ± SD)	81.94 ± 19.33	29.73 ± 27.96	$t = 7.781$	$p < 0.001$	$d = 2.172$
State anxiety (STAI-S percentile. M ± SD)	60.52 ± 26.48	15.77 ± 18.94	$t = 6.918$	$p < 0.001$	$d = 1.944$

Abbreviations: N = Sample size; M = Mean; SD = Standard deviation.

EEG data acquisition and preprocessing

EEG recording took place in a room fully equipped to minimize noise, electromagnetic interference, and environmental influences, providing an optimal setting for the procedure. Continuous EEG activity was recorded from 60 homogeneously distributed electrodes (10-10 system) mounted on a cap (ElectroCap International), referenced to both mastoids. Vertical and horizontal eye movements were monitored through electrooculographic (EOG)

recordings. The vertical EOG electrodes were positioned both below and above the left eye orbit, while the horizontal EOG electrodes were situated on the left and right orbital rims. Electrode impedances were maintained below 5 kΩ, and a bandpass filter of 0.1 – 50 Hz (3 dB points for -6 dB/octave roll-off) was applied to the recording amplifiers. Data were continuously digitized at a sampling rate of 250 Hz. Offline preprocessing was performed using a custom MATLAB R2023b [41] script containing EEGLAB v2023.1 [14] functions.

The EEG dataset used in this study was recorded as a part of a broader investigation involving event-related potentials (ERP), which falls beyond the scope of this article. In that experiment, participants were asked to perform a simple visual task that required categorizing a central digit as either above or below five, while peripheral stimuli were simultaneously presented (see, for example, Carretié [7]). Visual stimuli were displayed for 50 ms, with an interstimulus interval (ISI) of 3000 ms. During the ISI, participants stared at a fixation cross without engaging in any other activity. To define EEG segments free from task-related activity (i.e., RS signal), the maximum response time across all participants (850 ms) in the ERP paradigm was extracted, and an additional 500 ms latency was added. Epochs were then defined from 1350 ms after stimulus onset to 300 ms before the next stimulus onset. This resulted in a total of 4893 RS epochs with eyes open, each lasting 1350 ms, as per previous studies [13,17]. For preprocessing, ocular channels were removed from the data. The entire EEG recordings were digitally filtered using a bandpass finite impulse response filter (0.5 – 50 Hz). Eye blink artifacts were removed from the epoched data using Independent Component Analysis through EEGLAB's *runica* algorithm. Out of 60 total components, an average of 1 component (SD = 0.4) was removed for the HC group and 1.31 components (SD = 0.61) were removed for the FM group. No channels needed to be interpolated for any participant. To prune epochs containing artifacts, a semi-automatic trial rejection was performed based on voltage thresholds set at ± 100 µV. To further ensure there was no

lingering task activity in the data, epochs that still contained a response event were manually selected and removed. As a result, an average of 94.04 epochs (SD = 1.89) for the FM group and 94.42 epochs (SD = 2.86) for the HC group were retained for subsequent analyses. A summary of the EEG analysis pipeline is presented in Figure 1.

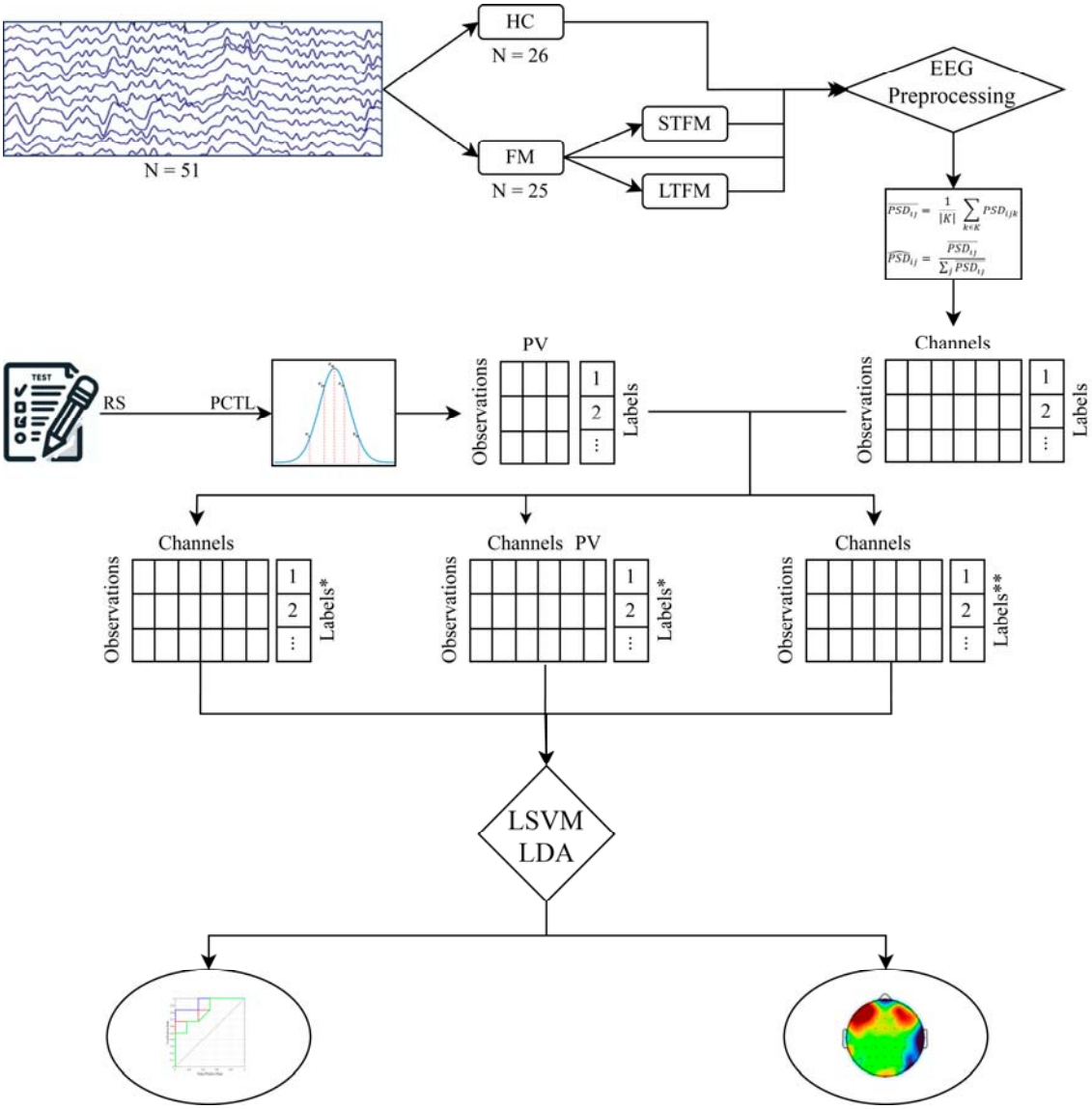

Figure 1 Pipeline of data processing and analyses. (*) indicates labels used for FM and HC comparison. (**) indicates labels used for STFM and LTFM comparison. Abbreviations: N = Sample size; HC = Healthy controls; FM = Fibromyalgia; STFM = Short-term fibromyalgia; LTFM = Long-term fibromyalgia; EEG = Electroencephalography; RS = Raw scores; PCTL = Percentile; PV = Psychometric values; LSVM = Linear support vector machine; LDA = Linear discriminant analysis.

Feature extraction

Building on previous studies examining RS data and patient diagnosis [1,31,47], the EEG data was decomposed into frequency bands. The resulting bands were as follows: delta (2 – 3.5 Hz), theta (4 – 7.5 Hz), alpha (8 – 12 Hz), alpha-1 (8 – 10 Hz), alpha-2 (10 – 12 Hz), beta (13 – 30 Hz), beta-1 (13 – 18 Hz), beta-2 (18.5 – 21 Hz), beta-3 (21.5 – 30 Hz), and gamma (30.5 – 44 Hz) [17,52]. These frequency bands were decomposed using the *ft_freqanalysis* function in FieldTrip [43], employing the multitaper method for performing fast Fourier transform with discrete prolate spheroid sequences on frequencies of interest ranging from 0.5 to 50 Hz, spaced at 0.74 Hz. The bands were then calculated for each channel and denominated as power spectral density (PSD). Once extracted, the PSD values were averaged for each channel (Equation 1) and then spectrally normalized (Equation 2) by dividing the PSD value at each channel by the total power of its corresponding observation [31]. This process was repeated for each frequency band.

$$\overline{PSD_{ij}} = \frac{1}{|K|} \sum_{k \in K} PSD_{ijk} \quad (1)$$

$$\widehat{PSD}_{ij} = \frac{\overline{PSD_{ij}}}{\sum_j \overline{PSD_{ij}}} \quad (2)$$

In addition to the frequency bands, psychometric values (PV), measured by self-reported anxiety scores derived from the STAI questionnaire, were also extracted. These values consisted of the percentile scores for each participant on both the trait and state anxiety scales. Prior to being used as additional features, these values were tested for significance between groups (Table 1) and trained separately from the PSD values. Significant PV were added as features along with PSD to examine their potential contribution to classification performance and to assess whether anxiety-related measures provide additional discriminative power between groups. Since PSD and PV are measured in different units,

they were normalized using the *zscore* function in MATLAB. Consequently, the training and testing datasets for comparing HC and FM were constructed using PSD, PV (STAI-S, STAI-T, and STAI-S + STAI-T), as well as combinations of PSD and PV (PSD + STAI-S, PSD + STAI-T, and PSD + STAI-S + STAI-T).

Additionally, the FM group was divided into two subgroups based on diagnostic length: 12 patients were included in the short-term fibromyalgia (STFM) group and 13 in the long-term fibromyalgia (LTFM) group. The median diagnostic length (92 months, $Q1$ = 64, $Q3$ = 107) served as the cutoff, with participants at the median value being randomly assigned to either group to ensure balance. A separate training and testing dataset was constructed using the PSD values from both groups to compare STFM and LTFM.

Classification models and performance evaluation

To distinguish between FM and HC, as well as between STFM and LTFM, linear discriminant analysis (LDA) and linear support vector machine (LSVM) models were trained. These models have previously been considered particularly well-suited for EEG decoding in cognitive neuroscience [23,48]. This is due to their simplicity, high computational efficiency, and ability to handle high-dimensional data [12,57]. Moreover, they exhibit high robustness to noise, which is especially useful since EEG data, even after preprocessing, tend to contain leftover noise signals [34].

To evaluate the performance of each classification model, we calculated accuracy (ACC), area under the receiver operating characteristic curve (AUC), recall, precision, and F1-score. To mitigate potential overfitting, models were trained using ten-fold cross-validation. This method splits the input data into ten folds, using one fold as the testing set and the remaining nine as the training set. This process was repeated ten times, and the average performance metric was recorded. Additionally, to account for data variability and assess the significance

of the observed performance metrics, the cross-validation procedure was repeated 1000 times, and the average performance metric was reported. As a baseline comparison, group labels were randomly permuted prior to model training.

Channel contribution analysis

Since our focus was on linear model variants, the weight of each channel after training can be interpreted as its contribution to the model's performance [28]. However, these weights should not be treated as straightforward indicators of brain activity since a channel with a large weight does not necessarily indicate the presence of the signal of interest, and a channel with a small weight may still carry relevant information [6,28]. To improve interpretability, the weight vectors were corrected using the method proposed by Haufe et al. [28], allowing them to be more accurately understood as sources of neural activity in space [37]. Furthermore, given that we considered the FM and STFM groups as true positive and the HC and LTFM groups as true negative in their respective analyses, positive weights indicate a higher contribution of a particular channel to correctly classify an observation as FM or STFM, while negative weights would reflect a greater contribution to classifying it as HC or LTFM.

Statistical Analyses

To assess statistical differences in age and anxiety scores between FM and HC groups, independent samples *t*-tests were performed. Differences in educational level were assessed using a chi-square (χ^2) test. To control for potential medication effects on brain activity within the FM group, a nonparametric permutation test was applied, given the small sample sizes and non-normal data distribution. Group-averaged PSD values were used for each channel and frequency band, with significance assessed via 5000 permutations and Monte Carlo *p*-values [39]. Finally, a paired samples *t*-test compared the classification performance

of LSVM and LDA to determine the most suitable model. All tests were carried out with a 95% confidence interval and all *t*-tests were two-tailed.

Results

PSD spatial distribution

Before model input, power spectral density (PSD) differences were calculated for the FM and HC groups, as well as for the STFM and LTFM groups. Spatial distribution is illustrated in Figure 2, and further detailed in Supplementary Tables 1 and 2.

Compared to HC, the FM group showed reduced PSD in prefrontal regions across delta, theta, and alpha bands, and in prefrontal and right occipitotemporal regions for beta and gamma bands. Conversely, they had increased PSD in left frontotemporal and occipital regions for delta and theta bands, and in frontal regions for beta and gamma bands.

When compared to LTFM, the STFM group exhibited reduced PSD in left frontocentral and occipital regions for delta and theta bands, while for beta and gamma bands, the reductions were more localized around the prefrontal and occipital regions. By contrast, they had increased PSD in frontotemporal regions for beta and gamma bands.

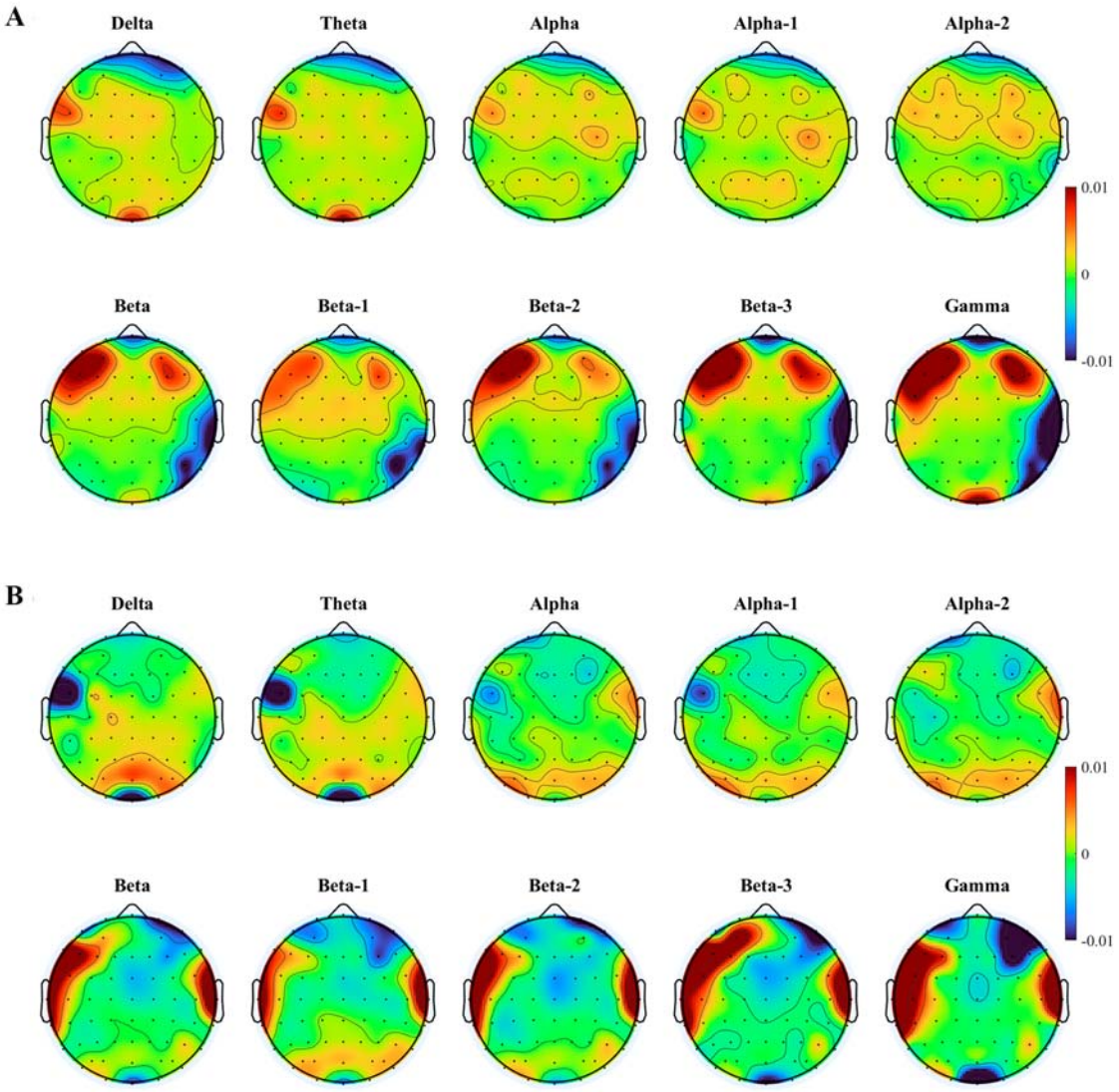

Figure 2 Topographic representation of scalp sites across frequency bands. (**A**) Differences in normalized PSD between FM and HC. (**B**) Differences in normalized PSD between STFM and LTFM.

Model performance

To select the best model, power spectral density (PSD) values from EEG data of FM and HC across frequency bands were used to train linear discriminant analysis (LDA) and linear support vector machine (LSVM) models. As a result, LSVM outperformed LDA in most frequency bands, except for the alpha band. A paired *t*-test confirmed that LSVM significantly outperformed LDA in these bands ($p < 0.01$) and was selected for all subsequent

analyses. Performance metrics are illustrated in Figure 3 and further detailed in Supplementary Table 3.

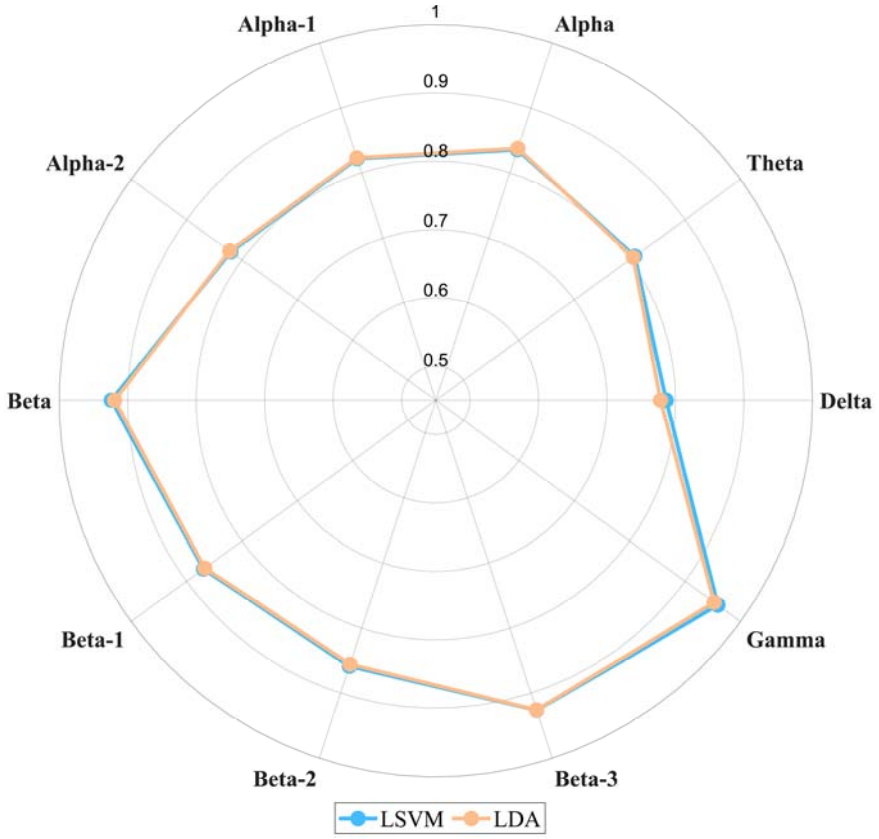

Figure 3 Classifier performance (AUC). Comparison across frequency bands using PSD values for LDA and LSVM models.

Classification using discriminative features of EEG data

EEG features and anxiety scores in FM classification

To distinguish HC from FM, power spectral density (PSD) from EEG data and psychometric values (PV) from the STAI questionnaire were used to train a linear support vector machine (LSVM) model. Performance across feature combinations is shown in Figure 4 and detailed in Supplementary Tables 4 and 5. The permuted label accuracy was approximately 0.5 for all frequencies, confirming the validity of the data.

With PSD alone the model distinguished well between groups, particularly in beta-3 (*ACC* = 0.87, *AUC* = 0.93) and gamma (*ACC* = 0.90, *AUC* = 0.96) bands. Including either state (PSD + STAI-S) or trait (PSD + STAI-T) anxiety further improved performance across all bands, achieving AUC values above 0.98 for both beta-3 and gamma bands. The best distinction was obtained by combining all features, especially in beta-3 (*ACC* = 0.99, *AUC* = 1.00) and gamma (*ACC* = 0.99, *AUC* = 1.00).

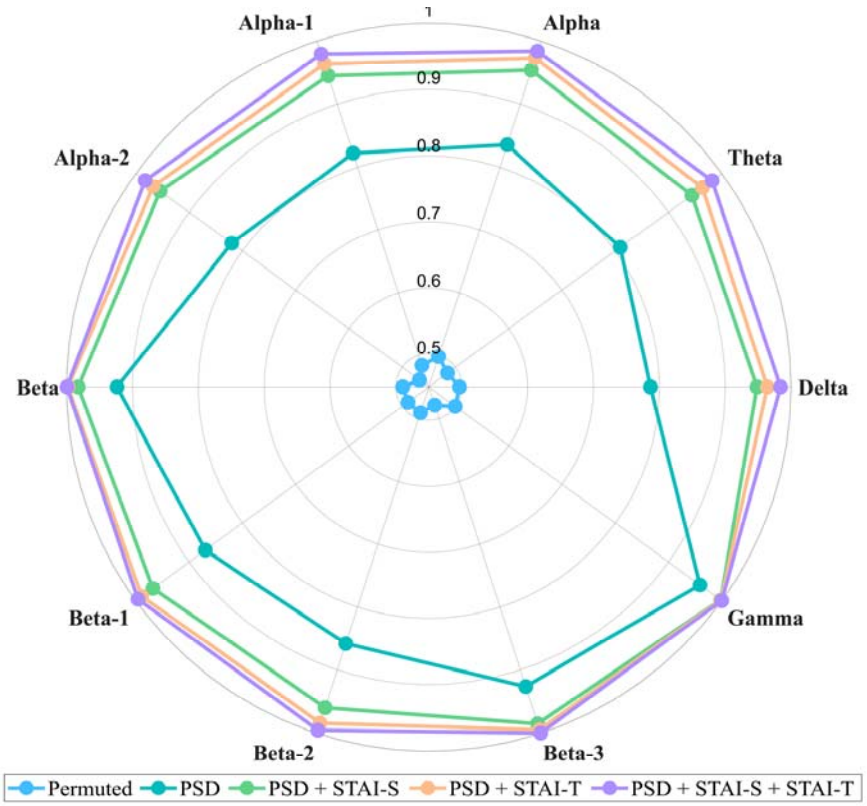

Figure 4 Classifier performance (AUC). Comparison across frequency bands for FM and HC.

Classifying STFM and LTFM using EEG features

To compare short-term fibromyalgia (STFM) and long-term fibromyalgia (LTFM) groups, power spectral density (PSD) from EEG data was used to train a linear support vector machine (LSVM) model. Model performance is shown in Figure 5 and further detailed in Supplementary Table 6.

The model successfully distinguished STFM from LTFM patients, particularly in beta-1 (*ACC* = 0.88, *AUC* = 0.95), beta-2 (*ACC* = 0.87, *AUC* = 0.95), beta-3 (*ACC* = 0.94, *AUC* = 0.98), and gamma (*ACC* = 0.98, *AUC* = 1.00) bands.

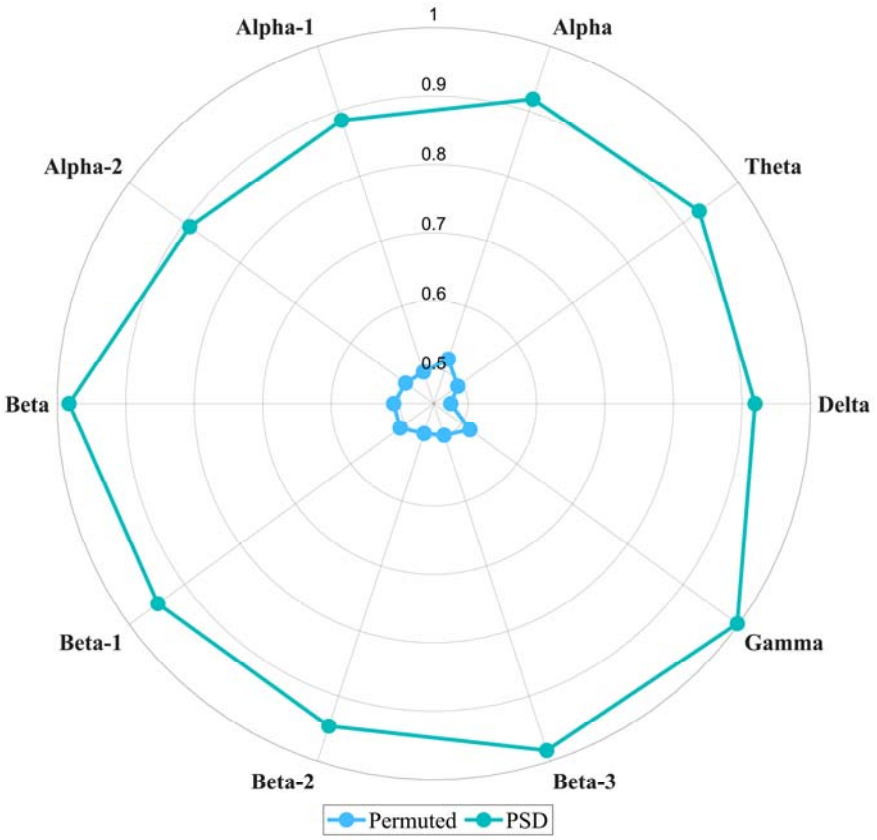

Figure 5. Classifier performance (AUC). Comparison across frequency bands for STFM and LTFM.

Channel contribution to group classification

To interpret the neural scalp sites contributing to classification, the correction method proposed by Haufe et al. [28] was applied to the weight matrix obtained after classification. This transformation provides a more accurate spatial representation of relevant neural activity across frequency bands distinguishing FM from HC, as well as STFM from LTFM. The corrected weight maps are shown in Figure 6, and detailed in Supplementary Tables 7 and 8.

In both comparisons, delta and theta exhibited similar spatial patterns in frontocentral and occipital regions. In the FM and HC comparison, prefrontal regions also contributed notably.

Alpha and alpha-1 activity were concentrated in left frontocentral regions across both comparisons, while alpha-2 was more prominent in right temporoparietal regions in the FM and HC comparison, and in left prefrontal and right temporal regions in the STFM and LTFM comparison. Notably, the entire alpha band showed strong prefrontal contributions in the FM and HC comparison. Beta and gamma activity in the FM and HC comparison were primarily associated with frontal, left frontocentral, and right parieto-occipital regions. Conversely, the comparison between STFM and LTFM revealed beta activity predominantly in right temporal areas, with beta-3 extending into left prefrontal regions, and gamma activity mainly in prefrontal, temporal, and occipital areas.

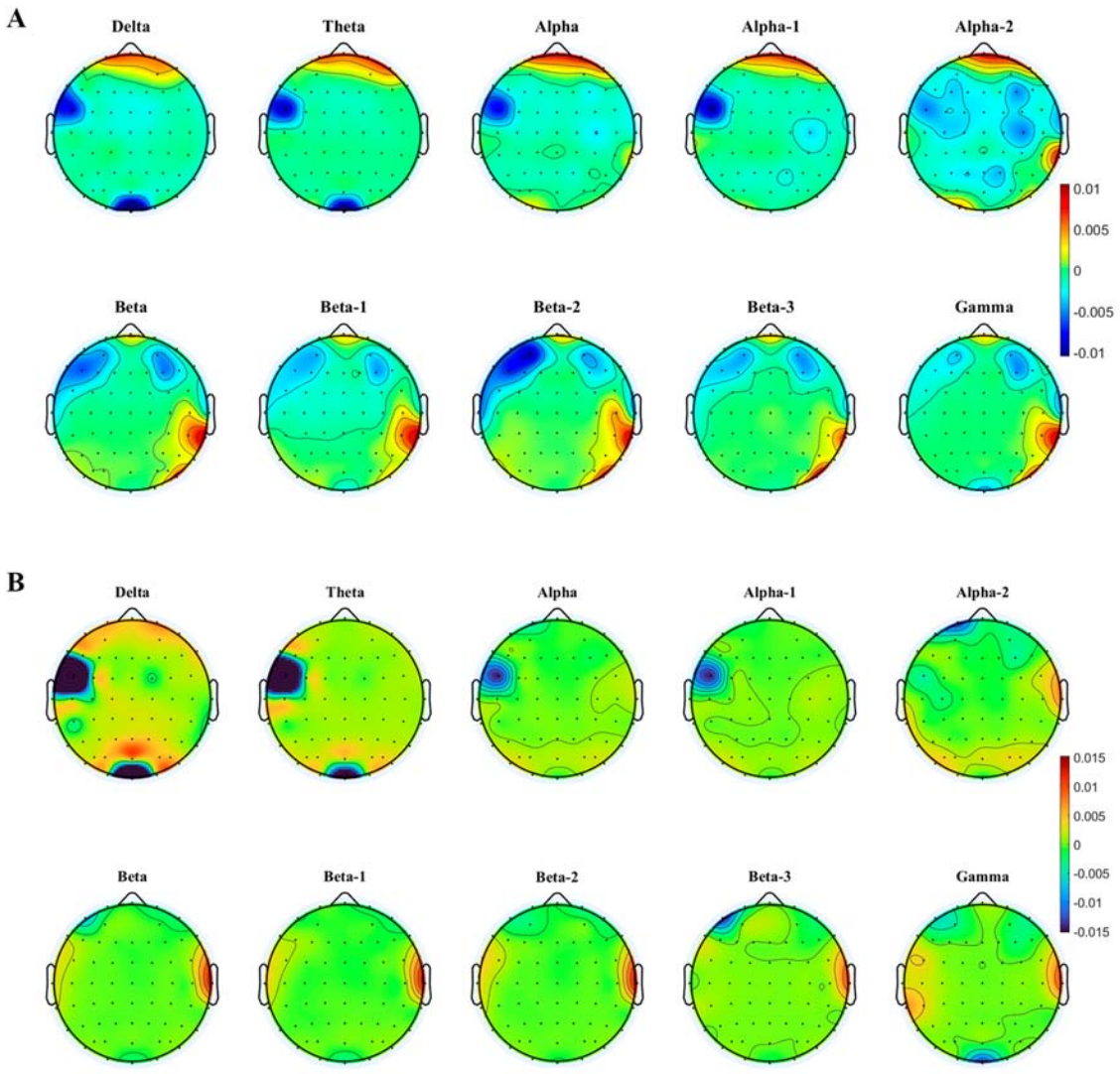

Figure 6 Topographic distribution of scalp site contributions across frequency bands. (**A**) Scalp site contributions in FM and HC. (**B**) Scalp site contributions in STFM and LTFM.

Medication effects on brain activity in the FM group

To assess potential medication effects on brain activity in FM patients, we conducted nonparametric permutation tests comparing mean power spectral density (PSD) values between medicated and non-medicated patients.

Channels with significant differences (i.e., $p < 0.05$) are illustrated in Figure 7 and detailed in Supplementary Table 9. None of these channels contributed meaningfully to the classification

models, except for channel AF7 in beta-2, beta-3, and gamma bands for the analgesics condition. For anxiolytics and antiepileptics/psycholeptics conditions, sample sizes (6 and 4 participants, respectively) were too small to conduct meaningful statistical analyses.

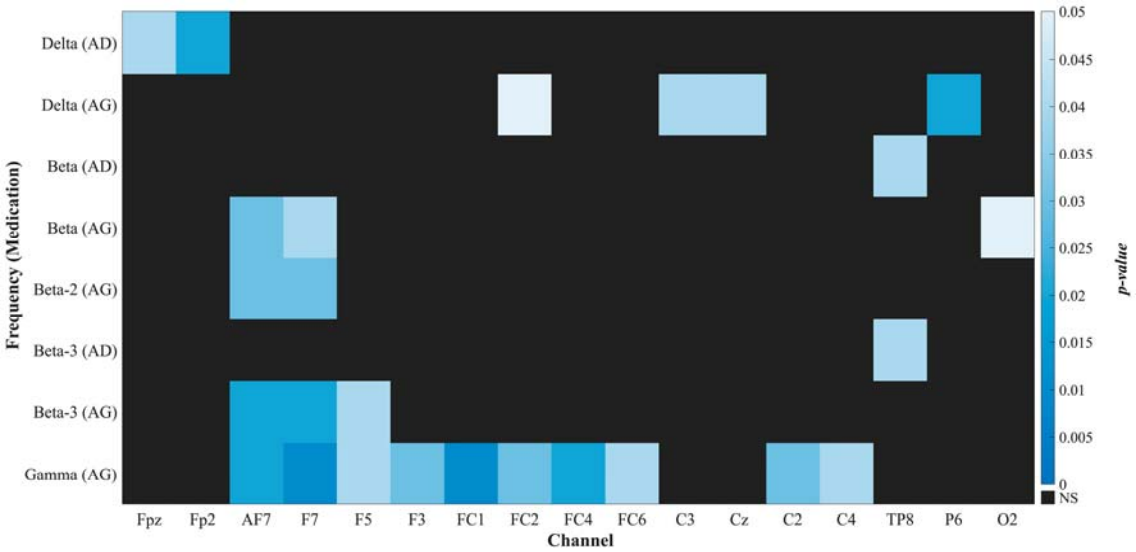

Figure 7 Heatmap of statistical differences in mean PSD values across frequency bands. Comparison between FM participants with and without medication use. Abbreviations: NS = Not Significant, AD = Antidepressants, AG = Analgesics.

Discussion

In the present study, we investigated abnormalities in EEG activity in fibromyalgia (FM) patients during open-eyes resting-state (RS). We applied a linear support vector machine (LSVM) model in three novel analyses. First, we trained the model with power spectral density (PSD) and anxiety scores to distinguish FM patients from healthy controls (HC). Second, we used diagnosis duration to distinguish between short-term (STFM) and long-term FM (LTFM) patients. Both analyses accurately differentiated groups across frequency bands. Third, we identified key scalp regions whose neural activity contributed most to the classification. This integrated EEG and psychometric data, linking brain activity to symptom duration and anxiety. By aligning our methodology with the study's objectives, we were able

to highlight the critical role these variables play in understanding the heterogeneity and complexity of FM.

Building on our integrated approach, we identified specific neural features enabling accurate classification of FM patients and HC. Notably, beta and gamma frequency bands emerged as the most discriminative. Within the beta band, particularly beta-3, classification performance was strongest, with scalp key contributions over frontal, right temporal, and right parieto-occipital regions. As the analysis was conducted in sensor space rather than source space, cortical interpretations should be done carefully. Nonetheless, brain areas situated under these scalp locations, such as the anterior insular, dorsolateral prefrontal, and secondary somatosensory cortices have been implicated in pain perception and its modulation [2,25,52]. Moreover, beta-3 activity has been linked to interactions between sensory, affective, and attentional circuits involved in pain processing [2]. Abnormal beta oscillations have been linked not only to pain processing but also to impairments in motor control, visual attention, and emotion regulation [3,4,16,26]. While research on gamma activity in nociplastic pain is limited, increased gamma oscillations have been associated with heightened pain sensitivity and enhanced attentional focus on somatosensory stimuli [2,27,50].

Although beta oscillations relate to pain processing and broader cognitive functions, alpha and theta bands are more directly linked to pain inhibition and cognitive control [17,52]. Specifically, previous studies report a negative correlation between pain levels and alpha power, indicating that chronic pain in FM patients may act as a persistent noxious stimulus that progressively diminishes alpha activity [40,52]. This aligns with our findings, where reduced alpha PSD in prefrontal regions significantly distinguishes FM from HC. Additionally, increased prefrontal theta PSD in FM might indicate diminished inhibitory control over pain processing. This dysregulation could contribute to maladaptive feedback loops in which pain is amplified and poorly modulated, as brain areas near these scalp

locations, such as the dorsolateral prefrontal and medial prefrontal cortices, are involved in these processes [17,30].

In addition to pain-related symptoms, emotional symptoms such as anxiety are common in FM patients and often more severe than in age-matched controls, contributing to reduced quality of life [8,9,29]. Consistent with recent studies involving heat pain [31], our model's performance improved greatly when combining either state or trait anxiety with PSD, achieving the highest accuracy when both anxiety scores were included. Notably, combining trait anxiety with PSD outperformed the combination of state anxiety with PSD. This aligns with previous research suggesting that although both state and trait anxiety can intensify pain perception in FM patients, trait anxiety shows a stronger association [22]. These findings highlight that integrating psychological and electrophysiological variables provides a more comprehensive understanding of FM by capturing both emotional and neural profiles, offering deeper insight than analyzing each independently.

Evidence from FM and other chronic pain conditions suggests that prolonged exposure to pain alters brain structures and disrupts functional connectivity [3–5,33,35,42,46]. Although determining symptom onset in FM is challenging, as diagnosis often occurs years after initial symptoms, EEG studies associate longer symptom duration with more pronounced neural alterations [2]. This is consistent with our finding of high classification accuracy across all frequency bands when comparing STFM and LTFM groups. Additionally, altered theta power within frontal, frontocentral, and parietal regions has been associated with ongoing tonic pain and fatigue in FM [17,53]. In our study, we observed significant contributions from left frontotemporal regions within the theta band, near these regions. Regarding other frequency bands, the observed patterns may indicate exacerbations due to prolonged exposure to FM symptoms in the same regions commonly affected in FM when compared to HC, particularly those involved in pain processing and cognitive control.

The current study has several potential limitations. Other contributing factors cannot be ruled out, and further research is needed to clarify these findings. For instance, although the channels showing significant differences did not substantially influence classification models, and analgesic use has not been reported to affect pain-related brain activity, its impact cannot be entirely dismissed. Additionally, while some results align with prior univariate studies, several key regions within specific frequency bands remain underexplored, prompting further investigation to better understand their role in FM-related neurophysiological alterations.

In sum, our findings reveal significant differences in RS-EEG activity between FM patients and HC, as well as between STFM and LTFM. Incorporating anxiety scores improved the model's discriminative ability, emphasizing the value of integrating both emotional and neural factors. Frequency-specific alterations, particularly in scalp regions consistently associated with pain processing and cognitive control, support the notion that FM involves disrupted neural mechanisms of pain. Furthermore, multivariate pattern analysis effectively addresses the research questions, providing deeper insights into the disorder's complexity. Building on prior work using traditional methods, this approach provides a clearer picture of the neural alterations associated with FM. Given the ease of acquiring RS-EEG in clinical settings, it may be valuable for clinicians and researchers to consider focusing on frequency bands that show the most promise in classification, such as beta and gamma bands. This could help advance the development of EEG based biomarkers for FM, ultimately improving diagnostic and therapeutic strategies for the disease.

Data availability statement

The data supporting the findings of this study are available in the OSF repository at

https://osf.io/gyk89/

Funding statement

This work was supported by grant PID2020-115463RB-I00 from the Ministerio de Ciencia e Innovación of Spain.

Conflict of Interest statement

The authors have no conflicts of interest to declare.

References

[1] Abdellatef E, Emara HM, Shoaib MR, Ibrahim FE, Elwekeil M, El-Shafai W, Taha TE, El-Fishawy AS, El-Rabaie E-SM, Eldokany IM, Abd El-Samie FE. Automated diagnosis of EEG abnormalities with different classification techniques. Med Biol Eng Comput 2023;61:3363–3385.

[2] Alves RL, Zortea M, Serrano PV, Brugnera Tomedi R, Pereira De Almeida R, Torres ILS, Fregni F, Caumo W. High-beta oscillations at EEG resting state and hyperconnectivity of pain circuitry in fibromyalgia: an exploratory cross-sectional study. Front Neurosci 2023;17:1233979.

[3] Apkarian AV, Sosa Y, Sonty S, Levy RM, Harden RN, Parrish TB, Gitelman DR. Chronic Back Pain Is Associated with Decreased Prefrontal and Thalamic Gray Matter Density. J Neurosci 2004;24:10410–10415.

[4] Baliki MN, Geha PY, Apkarian AV, Chialvo DR. Beyond Feeling: Chronic Pain Hurts the Brain, Disrupting the Default-Mode Network Dynamics. J Neurosci 2008;28:1398–1403.

[5] Bekkelund SI, Pierre-Jerome C, Husby G, Mellgren SI. Quantitative cerebral MR in rheumatoid arthritis. AJNR Am J Neuroradiol 1995;16:767–772.

[6] Blankertz B, Lemm S, Treder M, Haufe S, Müller K-R. Single-trial analysis and classification of ERP components — A tutorial. NeuroImage 2011;56:814–825.

[7] Carretié L. Exogenous (automatic) attention to emotional stimuli: a review. Cogn Affect Behav Neurosci 2014;14:1228–1258.

[8] Catalá P, Gutiérrez L, Écija C, Peñacoba C. Pathological Cycle between Pain, Insomnia, and Anxiety in Women with Fibromyalgia and its Association with Disease Impact. Biomedicines 2023;11:148.

[9] Cetingok S, Seker O, Cetingok H. The relationship between fibromyalgia and depression, anxiety, anxiety sensitivity, fear avoidance beliefs, and quality of life in female patients. Medicine 2022;101:e30868.

[10] Choe MK, Lim M, Kim JS, Lee DS, Chung CK. Disrupted Resting State Network of Fibromyalgia in Theta frequency. Sci Rep 2018;8:2064.

[11] Clauw DJ. Fibromyalgia: A Clinical Review. JAMA 2014;311:1547.

[12] Cortes C, Vapnik V. Support-vector networks. Mach Learn 1995;20:273–297.

[13] D'Croz-Baron DF, Bréchet L, Baker M, Karp T. Auditory and Visual Tasks Influence the Temporal Dynamics of EEG Microstates During Post-encoding Rest. Brain Topogr 2021;34:19–28.

[14] Delorme A, Makeig S. EEGLAB: an open source toolbox for analysis of single-trial EEG dynamics including independent component analysis. Journal of Neuroscience Methods 2004;134:9–21.

[15] Djoufack Nkengfack LC, Tchiotsop D, Atangana R, Louis-Door V, Wolf D. EEG signals analysis for epileptic seizures detection using polynomial transforms, linear discriminant analysis and support vector machines. Biomedical Signal Processing and Control 2020;62:102141.

[16] Engel AK, Fries P. Beta-band oscillations — signalling the status quo? Current Opinion in Neurobiology 2010;20:156–165.

[17] Fallon N, Chiu Y, Nurmikko T, Stancak A. Altered theta oscillations in resting EEG of fibromyalgia syndrome patients. European Journal of Pain 2018;22:49–57.

[18] Fernandes-Magalhaes R, Carpio A, Ferrera D, Peláez I, De Lahoz ME, Van Ryckeghem D, Van Damme S, Mercado F. Neural mechanisms underlying attentional bias modification in fibromyalgia patients: a double-blind ERP study. Eur Arch Psychiatry Clin Neurosci 2024;274:1197–1213.

[19] Fernandes-Magalhaes R, Ferrera D, Peláez I, Martín-Buro MC, Carpio A, De Lahoz ME, Barjola P, Mercado F. Neural correlates of the attentional bias towards pain-related faces in fibromyalgia patients: An ERP study using a dot-probe task. Neuropsychologia 2022;166:108141.

[20] Ferrera D, Gómez-Esquer F, Peláez I, Barjola P, Fernandes-Magalhaes R, Carpio A, De Lahoz ME, Díaz-Gil G, Mercado F. Effects of COMT Genotypes on Working Memory Performance in Fibromyalgia Patients. JCM 2020;9:2479.

[21] Ferrera D, Mercado F, Peláez I, Martínez-Iñigo D, Fernandes-Magalhaes R, Barjola P, Écija C, Díaz-Gil G, Gómez-Esquer F. Fear of pain moderates the relationship between self-reported fatigue and methionine allele of catechol-O-methyltransferase gene in patients with fibromyalgia. PLoS ONE 2021;16:e0250547.

[22] Galvez-Sánchez CM, Montoro CI, Duschek S, Reyes Del Paso GA. Depression and trait-anxiety mediate the influence of clinical pain on health-related quality of life in fibromyalgia. Journal of Affective Disorders 2020;265:486–495.

[23] Garrett D, Peterson DA, Anderson CW, Thaut MH. Comparison of linear, nonlinear, and feature selection methods for EEG signal classification. IEEE Trans Neural Syst Rehabil Eng 2003;11:141–144.

[24] Giorgi V, Sirotti S, Romano ME, Marotto D, Ablin JN, Salaffi F, Sarzi-Puttini P. Review Fibromyalgia: one year in review 2022. Clinical and Experimental Rheumatology 2022.

[25] González-Villar AJ, Triñanes Y, Gómez-Perretta C, Carrillo-de-la-Peña MT. Patients with fibromyalgia show increased beta connectivity across distant networks and microstates alterations in resting-state electroencephalogram. NeuroImage 2020;223:117266.

[26] Hauck M, Domnick C, Lorenz J, Gerloff C, Engel AK. Top-down and bottom-up modulation of pain-induced oscillations. Front Hum Neurosci 2015;9. doi:10.3389/fnhum.2015.00375.

[27] Hauck M, Lorenz J, Engel AK. Attention to Painful Stimulation Enhances γ-Band Activity and Synchronization in Human Sensorimotor Cortex. J Neurosci 2007;27:9270–9277.

[28] Haufe S, Meinecke F, Görgen K, Dähne S, Haynes J-D, Blankertz B, Bießmann F. On the interpretation of weight vectors of linear models in multivariate neuroimaging. NeuroImage 2014;87:96–110.

[29] Henao-Pérez M, López-Medina DC, Arboleda A, Bedoya Monsalve S, Zea JA. Patients With Fibromyalgia, Depression, and/or Anxiety and Sex Differences. Am J Mens Health 2022;16:15579883221110351.

[30] Henderson LA, Peck CC, Petersen ET, Rae CD, Youssef AM, Reeves JM, Wilcox SL, Akhter R, Murray GM, Gustin SM. Chronic Pain: Lost Inhibition? J Neurosci 2013;33:7574–7582.

[31] Hsiao F-J, Chen W-T, Pan L-LH, Liu H-Y, Wang Y-F, Chen S-P, Lai K-L, Wang S-J. Machine learning–based prediction of heat pain sensitivity by using resting-state EEG. Front Biosci (Landmark Ed) 2021;26:1537–1547.

[32] Hsiao F-J, Wang S-J, Lin Y-Y, Fuh J-L, Ko Y-C, Wang P-N, Chen W-T. Altered insula–default mode network connectivity in fibromyalgia: a resting-state magnetoencephalographic study. J Headache Pain 2017;18:89.

[33] Jin C, Yuan K, Zhao L, Zhao L, Yu D, Von Deneen KM, Zhang M, Qin W, Sun W, Tian J. Structural and functional abnormalities in migraine patients without aura. NMR in Biomedicine 2013;26:58–64.

[34] Khanam F, Hossain ABMA, Ahmad M. Electroencephalogram-based cognitive load level classification using wavelet decomposition and support vector machine. Brain-Computer Interfaces 2023;10:1–15.

[35] Kuchinad A, Schweinhardt P, Seminowicz DA, Wood PB, Chizh BA, Bushnell MC. Accelerated Brain Gray Matter Loss in Fibromyalgia Patients: Premature Aging of the Brain? J Neurosci 2007;27:4004–4007.

[36] Kumbhare D, Ahmed S, Watter S. A narrative review on the difficulties associated with fibromyalgia diagnosis. Therapeutic Advances in Musculoskeletal 2018;10:13–26.

[37] López-García D, Peñalver JMG, Górriz JM, Ruz M. MVPAlab: A machine learning decoding toolbox for multidimensional electroencephalography data. Computer Methods and Programs in Biomedicine 2022;214:106549.

[38] López-Solà M, Woo C-W, Pujol J, Deus J, Harrison BJ, Monfort J, Wager TD. Towards a neurophysiological signature for fibromyalgia. Pain 2017;158:34–47.

[39] Maris E, Oostenveld R. Nonparametric statistical testing of EEG- and MEG-data. Journal of Neuroscience Methods 2007;164:177–190.

[40] Martín-Brufau R, Gómez MN, Sanchez-Sanchez-Rojas L, Nombela C. Fibromyalgia Detection Based on EEG Connectivity Patterns. JCM 2021;10:3277.

[41] MATLAB. 2023. Available: https://www.mathworks.com/.

[42] McCrae C, O'Shea A, Boissoneault J, Vatthauer K, Robinson M, Staud R, Perlstein W, Craggs J. Fibromyalgia patients have reduced hippocampal volume compared with healthy controls. JPR 2015:47.

[43] Oostenveld R, Fries P, Maris E, Schoffelen J-M. FieldTrip: Open Source Software for Advanced Analysis of MEG, EEG, and Invasive Electrophysiological Data. Computational Intelligence and Neuroscience 2011;2011:1–9.

[44] Pujol J, Blanco-Hinojo L, Doreste A, Ojeda F, Martínez-Vilavella G, Pérez-Sola V, Deus J, Monfort J. Distinctive alterations in the functional anatomy of the cerebral cortex in pain-sensitized osteoarthritis and fibromyalgia patients. Arthritis Res Ther 2022;24:252.

[45] Pujol J, Macià D, Garcia-Fontanals A, Blanco-Hinojo L, López-Solà M, Garcia-Blanco S, Poca-Dias V, Harrison BJ, Contreras-Rodríguez O, Monfort J, Garcia-Fructuoso F, Deus J. The contribution of sensory system functional connectivity reduction to clinical pain in fibromyalgia. Pain 2014;155:1492–1503.

[46] Rodriguez-Raecke R, Niemeier A, Ihle K, Ruether W, May A. Structural Brain Changes in Chronic Pain Reflect Probably Neither Damage Nor Atrophy. PLoS ONE 2013;8:e54475.

[47] Ruiz De Miras J, Ibáñez-Molina AJ, Soriano MF, Iglesias-Parro S. Schizophrenia classification using machine learning on resting state EEG signal. Biomedical Signal Processing and Control 2023;79:104233.

[48] Sha'abani MNAH, Fuad N, Jamal N, Ismail MF. kNN and SVM Classification for EEG: A Review. In: Kasruddin Nasir AN, Ahmad MA, Najib MS, Abdul Wahab Y, Othman NA, Abd Ghani NM, Irawan A, Khatun S, Raja Ismail RMT, Saari MM, Daud MR, Mohd Faudzi AA, editors. InECCE2019. Lecture Notes in Electrical Engineering. Singapore: Springer Singapore, 2020, Vol. 632. pp. 555–565. doi:10.1007/978-981-15-2317-5_47.

[49] Spielberger CD, Gorsuch RL, Lushene EE. Manual del Cuestionario de Ansiedad Estado/Rasgo (STAI). TEA Ediciones, Madrid 1982.

[50] Stefani LC, Leite FM, Da Graça L. Tarragó M, Zanette SA, De Souza A, Castro SM, Caumo W. BDNF and serum S100B levels according the spectrum of structural pathology in chronic pain patients. Neuroscience Letters 2019;706:105–109.

[51] Thanh Nhu N, Chen DY-T, Kang J-H. Identification of Resting-State Network Functional Connectivity and Brain Structural Signatures in Fibromyalgia Using a Machine Learning Approach. Biomedicines 2022;10:3002.

[52] Villafaina S, Collado-Mateo D, Fuentes-García JP. Impact of Fibromyalgia on Alpha-2 EEG Power Spectrum in the Resting Condition: A Descriptive Correlational Study. BioMed Research International 2019;2019:1–6.

[53] Villafaina S, Collado-Mateo D, Fuentes-García JP, Domínguez-Muñoz FJ, Gusi N. Duration of the Symptoms and Brain Aging in Women with Fibromyalgia: A Cross-Sectional Study. Applied Sciences 2019;9:2106.

[54] Wolfe F, Clauw DJ, Fitzcharles M, Goldenberg DL, Katz RS, Mease P, Russell AS, Russell IJ, Winfield JB, Yunus MB. The American College of Rheumatology Preliminary Diagnostic Criteria for Fibromyalgia and Measurement of Symptom Severity. Arthritis Care & Research 2010;62:600–610.

[55] Wolfe F, Clauw DJ, Fitzcharles M-A, Goldenberg DL, Häuser W, Katz RL, Mease PJ, Russell AS, Russell IJ, Walitt B. 2016 Revisions to the 2010/2011 fibromyalgia diagnostic criteria. Seminars in Arthritis and Rheumatism 2016;46:319–329.

[56] Wolfe F, Smythe HA, Yunus MB, Bennett RM, Bombardier C, Goldenberg DL, Tugwell P, Campbell SM, Abeles M, Clark P, Fam AG, Farber SJ, Fiechtner JJ, Michael Franklin C, Gatter RA, Hamaty D, Lessard J, Lichtbroun AS, Masi AT, Mccain GA, John Reynolds W, Romano TJ, Jon Russell I, Sheon RP. The american college of rheumatology 1990 criteria for the classification of fibromyalgia. Arthritis & Rheumatism 1990;33:160–172.

[57] Yu C, Wang M. Survey of emotion recognition methods using EEG information. Cognitive Robotics 2022;2:132–146.

[58] Zafar R, Kamel N, Naufal M, Malik AS, Dass SC, Ahmad RF, Abdullah JM, Reza F. A study of decoding human brain activities from simultaneous data of EEG and fMRI using MVPA. Australas Phys Eng Sci Med 2018;41:633–645.